A Transformer Protection Relay Based on Induced Voltages

Yong-Cheol Kang* and Byung-Eun Lee*

Abstract - This paper describes a transformer protection relay based on induced voltages. The ratio of the induced voltages of the primary and secondary windings is equal to the turns ratio during normal operating conditions such as magnetic inrush, overexcitation, and steady state, but it differs from the turns ratio in the case of internal faults. For a single-phase and a three-phase Y-Y transformer, the induced voltages are estimated and the ratios are compared with the turns ratio. For three-phase Y-Δ transformers, the differences between the induced voltages are estimated to use the line currents because delta-winding currents are practically unavailable. The proposed relay is tested under various conditions such as magnetic inrush, internal winding faults, overexcitation, and different core characteristics. The results evidently indicate that the relay successfully discriminates internal faults from magnetic inrush and overexcitation. This paper concludes by implementing the relay into a TMS320C6701 digital signal processor and reports satisfactory results. The relay requires no hysteresis data and can reduce the operating time of a relay.

Keywords: Induced voltages, Turns ratio, Magnetic inrush, Remanent flux, and Low-pass filter.

Nomenclature

Symbols	Definition
v_1, v_2	Voltages (for 1 ϕ)
i_1, i_2	Currents (for 1 ϕ)
R_1, R_2	Winding resistances (for 1 ϕ)
L_{l1}, L_{l2}	Leakage inductances (for 1 ϕ)
e_1, e_2	Induced voltages (for 1 ϕ)
ϕ_m	Mutual flux
N_1, N_2	Number of windings (for 1 ϕ)
v_A, v_B, v_C	Voltages (Y-winding for 3 ϕ)
i_A, i_B, i_C	Currents (Y-winding for 3 ϕ)
v_{ab}, v_{bc}, v_{ca}	Voltages (Δ-winding for 3 ϕ)
i_{ab}, i_{bc}, i_{ca}	Winding currents (Δ-winding for 3 ϕ)
i_a, i_b, i_c	Line currents (Δ-winding for 3 ϕ)
R_A, R_B, R_C	Winding resistances (Y-winding for 3 ϕ)
L_{lA}, L_{lB}, L_{lC}	Leakage inductances (Y-winding for 3 ϕ)
e_A, e_B, e_C	Induced voltages (Y-winding for 3 ϕ)
R_{ab}, R_{bc}, R_{ca}	Winding resistances (Δ-winding for 3 ϕ)
L_{lab}, L_{lbc}, L_{lca}	Leakage inductances (Δ-winding for 3 ϕ)
e_{ab}, e_{bc}, e_{ca}	Induced voltages (Δ-winding for 3 ϕ)

1. Introduction

Current differential relays are widely used to detect internal winding faults in power transformers. To prevent malfunction during magnetic inrush and overexcitation, the relays use harmonic restraints [1]. Generally, the increase in the voltage of a transmission system and length of a transmission line can make the noise frequency contained in relaying signals low when a fault occurs. Underground cables or large capacitor banks in particular can cause the resonating characteristic of the frequency component near the power frequency [2].

Some researches that avoid dependence on the harmonic components in a differential current have been reported [3–5]. They use electro-magnetic differential equations and have very fast operating speeds. However, some of these algorithms [3, 4] use winding currents, which are practically unavailable. Inagaki et al. [4] use some nonlinear elements. However, the nonlinear characteristics depend on the operating conditions of the core; thus, difficulties may arise in determining the values of the elements.

Sachdev et al. [5] use an algorithm that uses only linear elements. For a three-phase Y-Δ transformer, the algorithm decomposes the delta winding current into two components i.e., non-circulating and circulating components. An alternative procedure of estimating terms involving the latter is used and some approximations are made [5].

In a previous paper [6], we described the basic principles of a transformer protective relaying algorithm using the ratio of the induced voltages (RIV). This algorithm uses a mathematical approach to use line currents. The RIV is the same as the turns ratio except for internal faults. However, because this algorithm uses the backward Euler method for approximating the differentiation terms when calculating

* Division of Electronics and Information Engineering, Chonbuk National Univ., NPTC Kang (yckang@moak.chonbuk.ac.kr, mpec @netian.com)

Received January 14, 2003 ; Accepted April 23, 2003

the induced voltages, large errors may be caused when it is applied to a real system.

This paper describes the extensive study of the algorithm described in our previous paper [6] and uses a method for damping the numerical oscillation with a parallel damping resistance. The proposed relay was tested under various conditions, i.e., magnetic inrush, internal winding faults, overexcitation, and different core characteristics. A second-order Butterworth filter was designed as an anti-aliasing low-pass filter. This paper concludes by implementing the algorithm into a TMS320C6701 digital signal processor (DSP).

2. A Transformer Protection Relay Based on Induced Voltages

This section briefly describes a transformer protective relaying algorithm in our previous paper [6].

2.1 A two-winding single-phase transformer

Fig. 1 shows a two-winding single-phase transformer. In the case of no internal fault, v_1 and v_2 can be given by

$$v_1 = R_1 i_1 + L_{l1}\frac{di_1}{dt} + e_1 \tag{1}$$

$$v_2 = -R_2 i_2 - L_{l2}\frac{di_2}{dt} + e_2 . \tag{2}$$

e_1 and e_2 can be obtained from (1) and (2). Defining the RIV gives

$$RIV \equiv \frac{e_1}{e_2} . \tag{3}$$

For the steady state, the RIV at any instant is equal to the turns ratio (N_1/N_2) except for $e_1 = 0$ or $e_2 = 0$. Moreover, for magnetic inrush and overexcitation, the RIV is equal to N_1/N_2 even though e_1 and e_2 are non-sinusoidal and severely distorted. For internal faults, the RIV differs from N_1/N_2.

From this point, the RIV of (3) can be used for detecting an internal fault. However, as e_1 and e_2 are instantaneous values and pass through zero, the RIV is not always equal to N_1/N_2. Thus, this paper employs the Detector in the form of (4) rather than (3). If (4) is equal to zero, the transformer is not faulted; if it is non-zero, it is. The Detector evaluates the percent difference between the two estimated induced voltages.

$$Detector = \frac{e_1 - \frac{N_1}{N_2}e_2}{\sqrt{2}V_1} \times 100\% \tag{4}$$

where V_1 is the primary rated voltage.

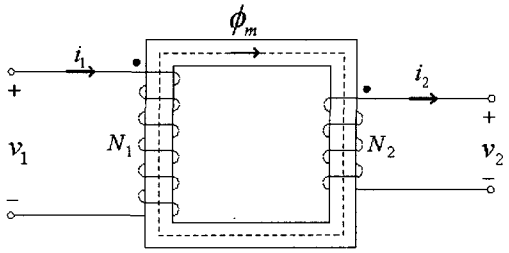

Fig. 1 A two-winding single-phase transformer

2.2 A two-winding three phase Y-Δ transformer

Fig. 2 shows the connections of primary and secondary windings for a three-phase Y-Δ transformer. Primary and secondary voltages can be represented by (5)–(10).

$$v_A = R_A i_A + L_{lA}\frac{di_A}{dt} + e_A \tag{5}$$

$$v_B = R_B i_B + L_{lB}\frac{di_B}{dt} + e_B \tag{6}$$

$$v_C = R_C i_C + L_{lC}\frac{di_C}{dt} + e_C \tag{7}$$

$$v_{ab} = R_{ab} i_{ab} + L_{lab}\frac{di_{ab}}{dt} + e_{ab} \tag{8}$$

$$v_{bc} = R_{bc} i_{bc} + L_{lbc}\frac{di_{bc}}{dt} + e_{bc} \tag{9}$$

$$v_{ca} = R_{ca} i_{ca} + L_{lca}\frac{di_{ca}}{dt} + e_{ca} \tag{10}$$

While e_A, e_B, and e_C can be obtained from (5)–(7), e_{ab}, e_{bc}, and e_{ca} cannot be calculated directly from (8)–(10) because i_{ab}, i_{bc} and i_{ca} are unavailable. On the contrary, i_a, i_b and i_c are always available. Thus, in this paper, to use i_a, i_b and i_c, the following relations are employed.

$$i_{ca} - i_{ab} = i_a , \quad i_{ab} - i_{bc} = i_b , \quad i_{bc} - i_{ca} = i_c \tag{11}$$

In addition, in the case of no internal fault, the following assumptions are possible.

$$R_{ab} \approx R_{bc} \approx R_{ca} = R , \quad L_{lab} \approx L_{lbc} \approx L_{lca} = L_l \tag{12}$$

Subtracting (8) from (10), (9) from (8), and (10) from (9) yields

$$e_{ca} - e_{ab} = v_{ca} - v_{ab} - Ri_a - L_l\frac{di_a}{dt} \tag{13}$$

$$e_{ab} - e_{bc} = v_{ab} - v_{bc} - Ri_b - L_l \frac{di_b}{dt} \quad (14)$$

$$e_{bc} - e_{ca} = v_{bc} - v_{ca} - Ri_c - L_l \frac{di_c}{dt}. \quad (15)$$

Though each of e_{ab}, e_{bc} and e_{ca} cannot be calculated, their differences can be calculated. The corresponding terms to (13)–(15) can be obtained from (5)–(7).

$$e_C - e_A = v_C - v_A - (R_C i_C - R_A i_A) - \left(L_{lC} \frac{di_C}{dt} - L_{lA} \frac{di_A}{dt} \right) \quad (16)$$

$$e_A - e_B = v_A - v_B - (R_A i_A - R_B i_B) - \left(L_{lA} \frac{di_A}{dt} - L_{lB} \frac{di_B}{dt} \right) \quad (17)$$

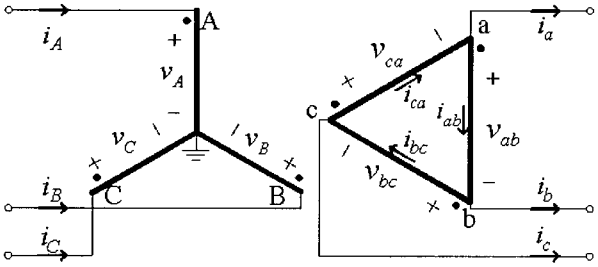

Fig. 2 A two-winding three-phase Y-Δ transformer

$$e_B - e_C = v_B - v_C - (R_B i_B - R_C i_C) - \left(L_{lB} \frac{di_B}{dt} - L_{lC} \frac{di_C}{dt} \right) \quad (18)$$

For a Y-Δ transformer, if no internal fault occurs, the following relationships are valid.

$$\frac{e_A}{e_{ab}} = \frac{N_1}{N_2}, \quad \frac{e_B}{e_{bc}} = \frac{N_1}{N_2}, \quad \frac{e_C}{e_{ca}} = \frac{N_1}{N_2} \quad (19)$$

While e_A, e_B and e_C can be calculated, e_{ab}, e_{bc} and e_{ca} cannot. Thus, (19) cannot be applied to the Detector. In this paper, in the case of a three-phase Y-Δ transformer, (20) is used for detectors. Equation (19) is a necessary and sufficient condition of (20). Its proof was shown in our previous work [6].

$$\frac{e_C - e_A}{e_{ca} - e_{ab}} = \frac{N_1}{N_2}, \frac{e_A - e_B}{e_{ab} - e_{bc}} = \frac{N_1}{N_2}, \frac{e_B - e_C}{e_{bc} - e_{ca}} = \frac{N_1}{N_2} \quad (20)$$

Consequently, the three Detectors for a Y-Δ transformer can be given by

$$Detector\ 1 = \frac{(e_C - e_A) - \frac{N_1}{N_2}(e_{ca} - e_{ab})}{\sqrt{2}V_{CA}} \times 100\% \quad (21)$$

$$Detector\ 2 = \frac{(e_A - e_B) - \frac{N_1}{N_2}(e_{ab} - e_{bc})}{\sqrt{2}V_{AB}} \times 100\% \quad (22)$$

$$Detector\ 3 = \frac{(e_B - e_C) - \frac{N_1}{N_2}(e_{bc} - e_{ca})}{\sqrt{2}V_{BC}} \times 100\% \quad (23)$$

Table 1 shows the rule for detecting internal faults and the faulted phase from the Detectors of (21), (22), and (23) for a three-phase Y-Δ transformer.

Table 1 A rule for detecting a fault and the faulted phase

Detector 1	Detector 2	Detector 3	Fault detection	
≈ 0	≈ 0	≈ 0	No internal fault	
≠ 0	≠ 0	≈ 0	A phase	Internal fault
≈ 0	≠ 0	≠ 0	B phase	
≠ 0	≈ 0	≠ 0	C phase	
Other cases			Internal fault	

3. Case studies

Fig. 3 shows the model system studied in this paper. A two-winding three-phase Y-Δ transformer (154kV/12.7kV, 55 MVA) is used for data generation using EMTP, and the sampling rate of 32 samples/cycle is employed. A method for modeling an internal winding fault [7] is used to model turn-to-ground and turn-to-turn winding faults.

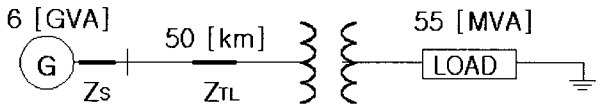

Fig. 3 The model system studied

To model hysteresis characteristics of the core for magnetic inrush and overexcitation, the type-96 element is used and the saturation point of (40 A, 334 Vs), where 334 Vs corresponds to 89 kV, is selected to use HYSDAT, a subroutine of EMTP.

The stop-band cut-off frequency of an anti-aliasing low-pass filter is selected as 960 Hz, which is the half the sampling frequency. All the voltages and currents are passed through the second-order Butterworth filter with the gain of 0.1 at 960 Hz.

Equations (13)–(18) contain differentiation terms, which should be approximated numerically to calculate the Detectors. Among the approximation methods using the two successive sample points, the trapezoidal rule causes a smaller error than the backward Euler method, but it can cause

numerical oscillation. Thus, in this paper, the differentiation terms are approximated by the trapezoidal rule in the form of (24) [8], a method for damping the numerical oscillation with a parallel damping resistance, R_P, as shown in Fig. 4.

$$v_L(t) = \frac{1}{\frac{\Delta t}{2L} + \frac{1}{R_P}}\{i(t) - i(t-\Delta t)\} - \frac{R_P - \frac{2L}{\Delta t}}{R_P + \frac{2L}{\Delta t}} v(t-\Delta t) \quad (24)$$

R_P is calculated using (25) as suggested in [8].

$$R_P = \frac{20}{3}\frac{2L}{\Delta t} \quad (25)$$

The performance of the proposed relay was verified in various conditions, such as magnetic inrush, internal winding faults, overexcitation, and different core characteristics.

3.1 Magnetic inrush

The magnitude of inrush currents depends on energization angle, a remanent flux in the core, and a load current. Thus, inrush current data are generated by varying these three parameters, and Table 2 shows the conditions for magnetic inrush data generation. Among them, the results of the two cases are shown.

Table 2 Conditions for magnetic inrush data generation

Energization angle (deg)	0, 90
Remanent flux (%)	0, 30, 50, 80
Load	No load, full load

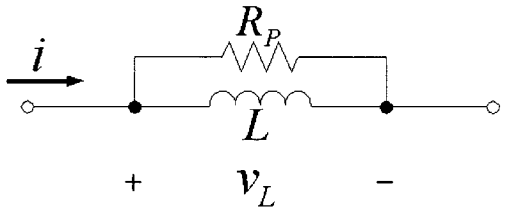

Fig. 4 Inductance model for the parallel damping

Case 1: Energization angle of 0 deg, 80% remanent flux, no load

Figs. 5–7 show the results for Case 1. The energization angle of 0 deg and 80% remanent flux cause very large inrush currents in the primary windings (Fig. 5). Primary and secondary voltages are severely distorted (Fig. 5). With the currents and voltages of Fig. 5, the left-hand sides of (13)–(18) are estimated.

Two corresponding terms in the three Detectors are shown in Fig. 6. For example, Fig. 6a shows $e_C - e_A$ and $N_1/N_2(e_{ca} - e_{ab})$ of Detector 1 estimated from (16) and (13), respectively. As expected, they are non-sinusoidal and severely distorted. However, the two estimated induced voltage differences are nearly the same even though inrush currents are very large and voltages are severely distorted.

The threshold for the Detectors can be determined by considering numerical error and sensitivity of a relay. In this paper, the threshold is set to 5% and a security counter is used for preventing maloperation due to transients. If the Detector is greater than 5%, the security counter is increased by 1; otherwise, it is decreased by 1. In addition, if the counter is less than 0, it is reset to 0. If the counter exceeds 4, the trip signal is activated. Fig. 7 shows the three Detectors and the trip signal. Since all the Detectors are less than 5%, no trip signal is activated.

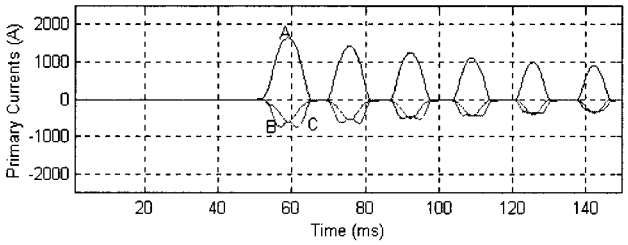

(a) Primary currents (i_A, i_B, i_C)

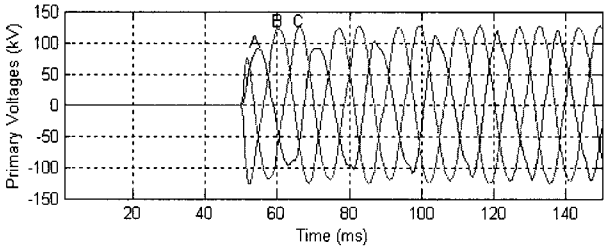

(b) Primary voltages (v_A, v_B, v_C)

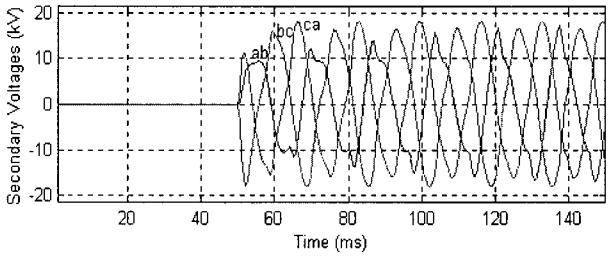

(c) Secondary voltages (v_{ab}, v_{bc}, v_{ca})

Fig. 5 Three-phase currents and voltages in Case 1

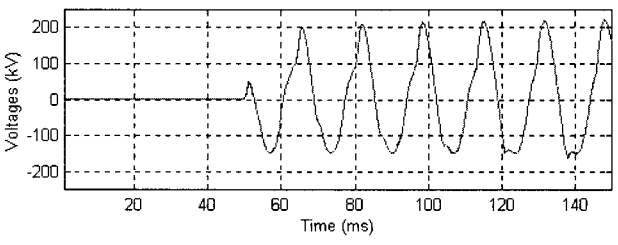

(a) e_C - e_A and $N_1/N_2(e_{ca}$ - $e_{ab})$ of Detector 1

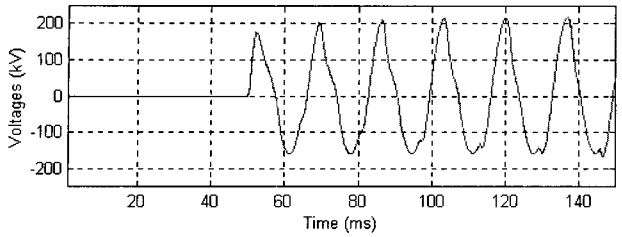

(b) $e_A - e_B$ and $N_1/N_2(e_{ab} - e_{bc})$ of Detector 2

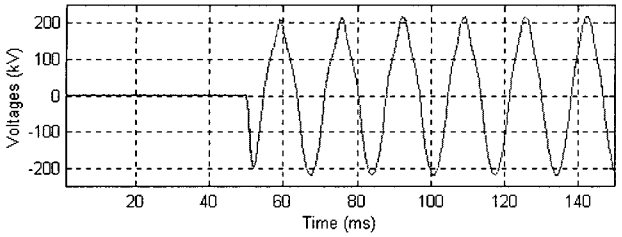

(c) $e_B - e_C$ and $N_1/N_2(e_{bc} - e_{ca})$ of Detector 3

Fig. 6 Estimated induced voltage differences in Case 1

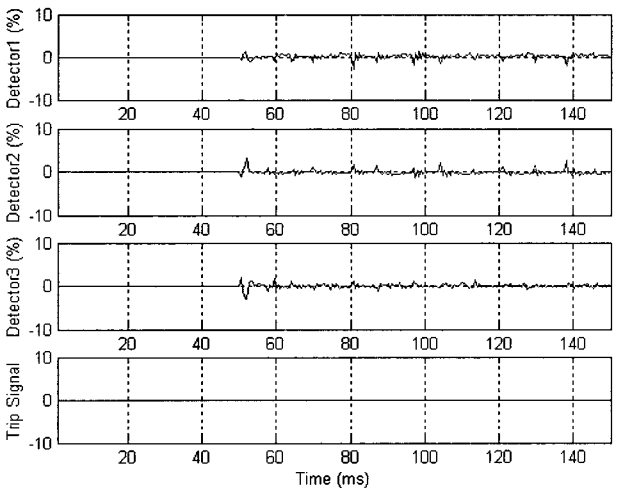

Fig. 7 Detectors and the trip signal in Case 1

Case 2: Energization angle of 0 deg, 80 % remanent flux, full load

Figs. 8 and 9 show that the results for Case 2 are identical to those for Case 1 except under a full load. Since a full load is connected, secondary currents flow as shown in Fig. 8b. Because of the load current, the primary currents have larger values when unsaturated than the Case 1. The peak value of the inrush current is similar to the Case 1. In addition, the primary and secondary voltages are severely distorted as in Case 1.

The estimated induced voltage differences from the distorted current and voltages of Fig. 8 are also nearly the same and thus the three Detectors have very small values as in Case 1. Thus, no trip signal is issued as shown in Fig. 9.

The results of the two cases evidently indicate that the proposed relay accurately estimates the induced voltage differences even though currents and voltages are severely distorted because of a high remanent flux and a load.

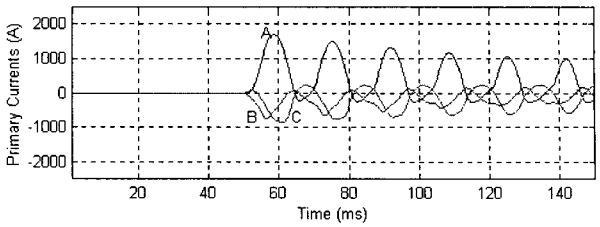

(a) Primary currents (i_A, i_B, i_C)

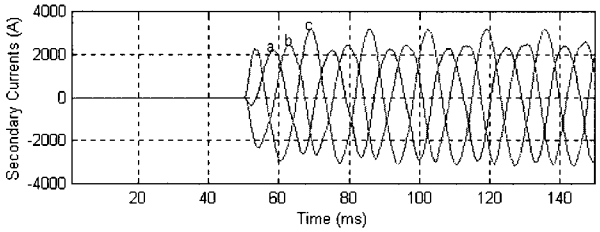

(b) Secondary currents (i_a, i_b, i_c)

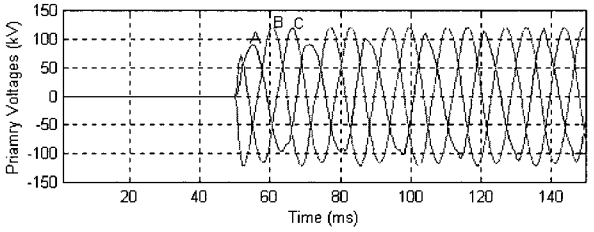

(c) Primary voltages (v_A, v_B, v_C)

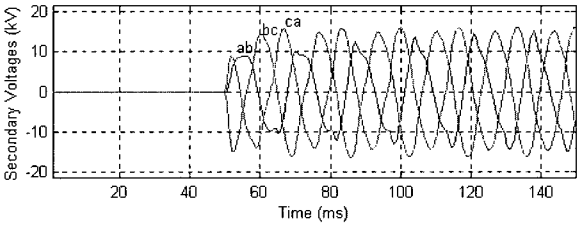

(d) Secondary voltages (v_{ab}, v_{bc}, v_{ca})

Fig. 8 Three phase currents and voltages in Case 2

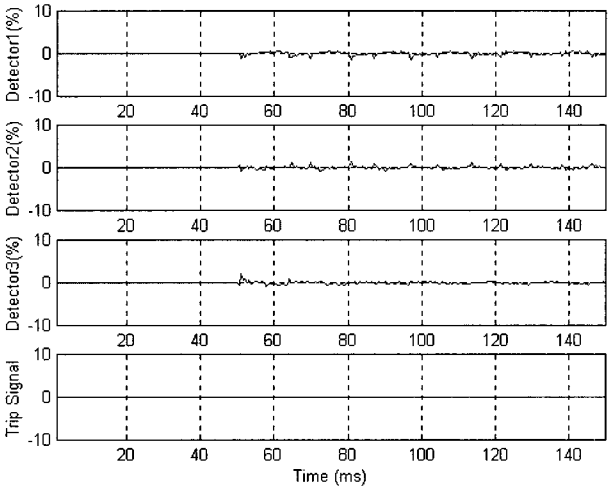

Fig. 9 Detectors and the trip signal in Case 2

3.2 Internal winding faults

Various internal winding fault data on the B phase in the

primary winding are generated by changing the type of a fault and used to test the proposed algorithm. The test results of the two cases are shown.

Case 3: A turn-to-ground fault, located 60 % from the neutral winding end and at 0 deg inception angle

Case 4: A turn-to-turn fault, located between 20% and 30% and at 0 deg inception angle

Figs. 10 and 11 show the three Detectors and the trip signals for Cases 3 and 4, respectively. As expected, in case of internal winding faults, the estimated induced voltage differences of the primary and secondary windings fail to correspond and thus the Detectors have values larger than 5%. Since a fault occurs on B phase, the Detector 2 and Detector 3 exceed 5%. Because the Detectors in Case 3 have larger values than in Case 4, the trip signal for Case 3 is issued faster than Case 4. The trip signal is issued 2.6 ms after fault occurrence. In Case 4, this delay is increased to 5.2 ms.

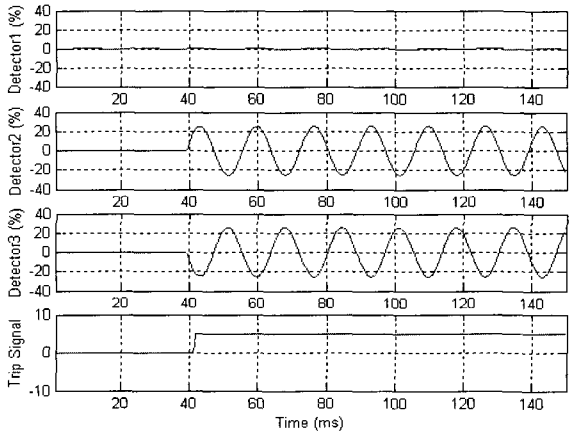

Fig. 10 Detectors and the trip signal in Case 3

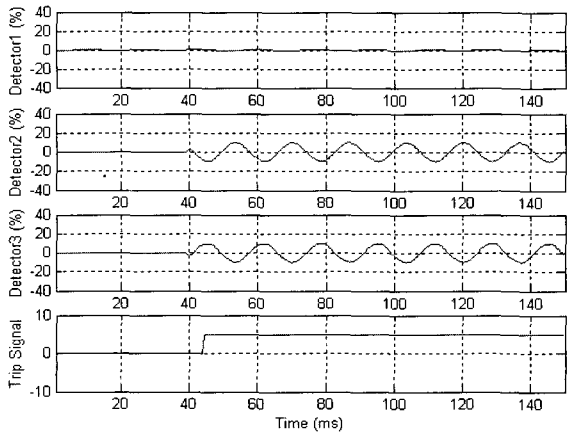

Fig. 11 Detectors and the trip signal in Case 4

3.3 Overexcitation

Case 5: Overvoltage of 150% applied, full load

The proposed relay was tested in the case of stationary overexcitation. Figs. 12 and 13 show the results. As an extreme case, 150% of the primary rated voltage (133 kV) is applied. The primary currents and voltages are distorted and contain harmonic components as shown in Fig. 12. However, the relay correctly estimates the induced voltage differences and thus no trip signal is issued (Fig. 13).

3.4 Different core characteristics

Because the relay requires no hysteresis data, it can detect internal faults even if core characteristics are changed. To validate this statement, tests are performed with different core characteristics, i.e., the excitation currents at the saturation points were changed without modifying the flux linkage. The winding resistance and leakage inductance remain unchanged.

Case 6: Energization angle of 0 deg, 80 % remanent flux, no load, saturation point of (80 A, 334 Vs)

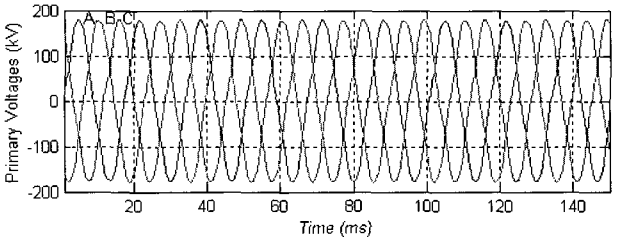

(a) Primary voltages

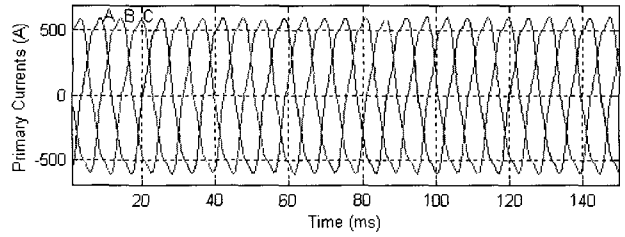

(b) Primary currents

Fig. 12 Primary voltages and currents in Case 5

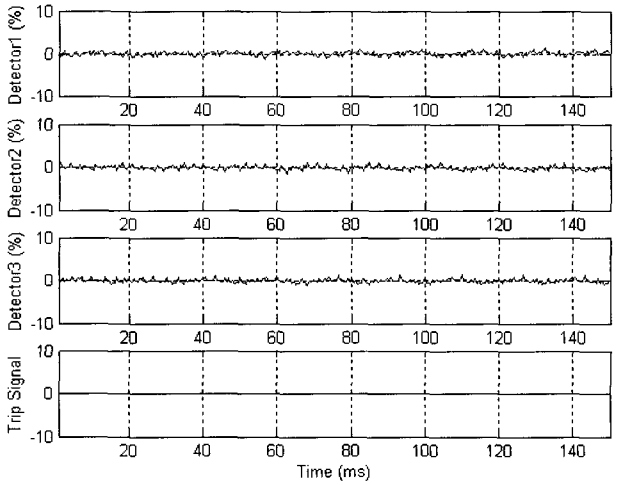

Fig. 13 Detectors and the trip signal in Case 5

Fig. 14 shows the results for Case 6; it is identical to Case 1 except for the current of the saturation point. In this case, although inrush currents are larger and thus voltages are more distorted than in Case 1, the Detectors are small and thus no trip signal is issued. The results show that the algorithm accurately estimates the induced voltage differences in the case of different core characteristics.

4. Hardware Implementation Test

Fig. 15 shows the configuration of the hardware implementation of the relay. The relay board uses the TMS320C6701 DSP. The analog signals fed from the PCL-727 digital-to-analog conversion (D/A) board, which has 12-bit D/A output channels, are converted into digital data at the sampling rate of 32 s/c. Second-order Butterworth low-pass filters are used with the same stop-band cut-off frequency as the simulation and are Sallen & Key active filters.

Figs. 16 and 17 show the results for Case 1. Because of the noise signal caused by hardware, the errors are bigger than the simulation results (Fig. 16). However, the algorithm performs successfully with the same threshold value of 5% and security counter of 4 as in the simulation (Fig. 17).

Fig. 18 shows the results for Case 3. The trip signal is activated 2.6 ms after fault occurrence although the errors are increased more than in the simulation results.

The above results clearly show that the relay performs properly even with errors larger than those used in the simulation when it is implemented into a TMS320C6701 DSP.

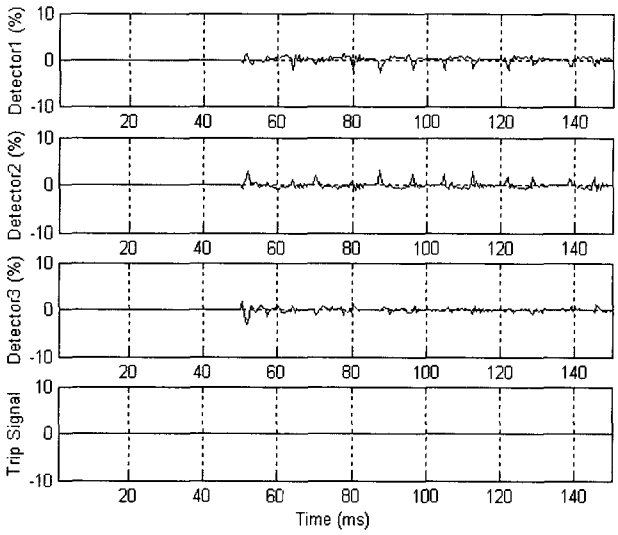

Fig. 14 Detectors and the trip signal in Case 6

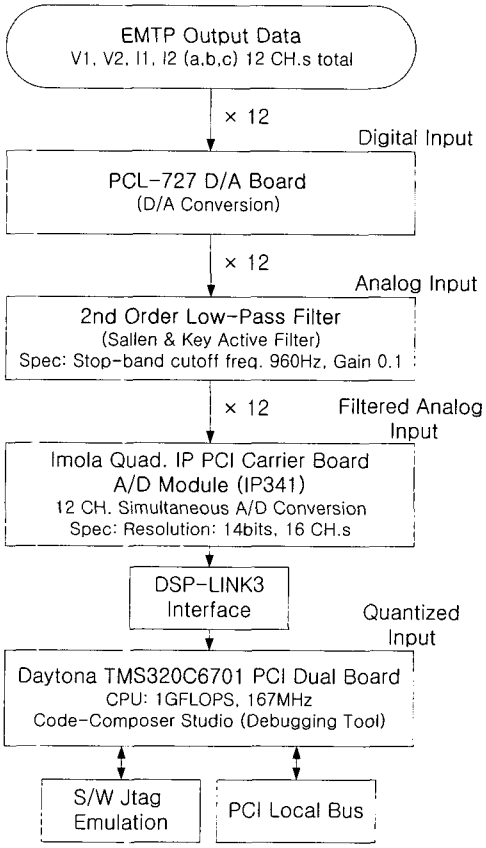

Fig. 15 The configuration of hardware implementation

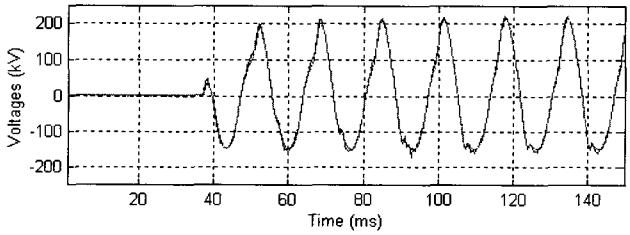

(a) $e_C - e_A$ and $N_1/N_2(e_{ca} - e_{ab})$ of Detector 1

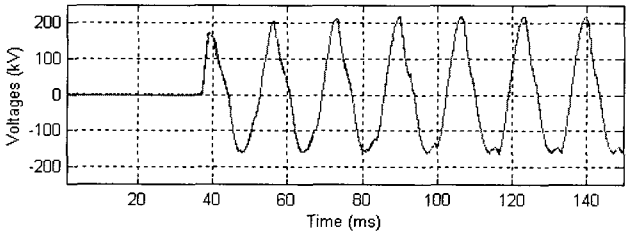

(b) $e_A - e_B$ and $N_1/N_2(e_{ab} - e_{bc})$ of Detector 2

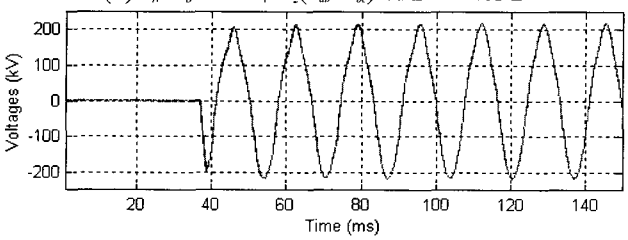

(c) $e_B - e_C$ and $N_1/N_2(e_{bc} - e_{ca})$ of Detector 3

Fig. 16 Estimated induced voltage differences in Case 1

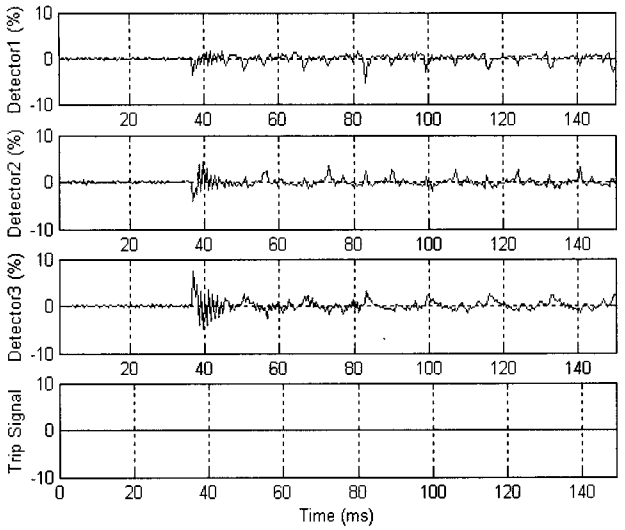

Fig. 17 The results of hardware implementation in Case 1

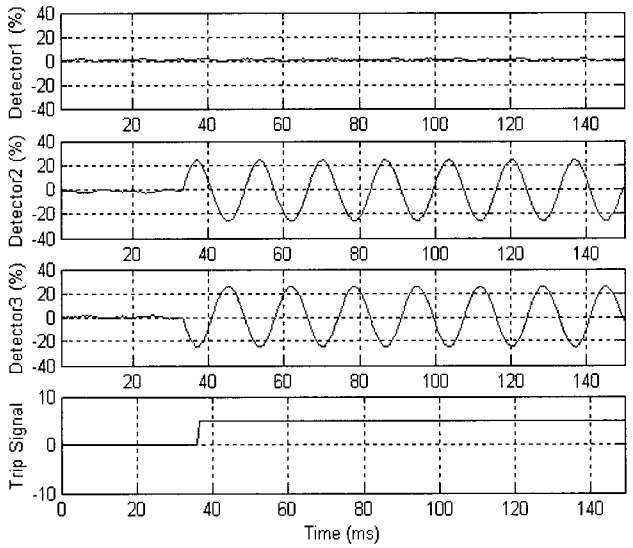

Fig. 18 The results of hardware implementation in Case 3

5. Conclusion

This paper proposes a transformer protection relay based on the induced voltages. Even when the currents and voltages are severely distorted, the proposed relay estimates the induced voltage differences of the primary and secondary windings and discriminates internal faults from magnetic inrush and overexcitation. Various test results clearly demonstrate that the relay performs well in cases of magnetic inrush, overexcitation, and different core characteristics. In addition, it detects internal faults less than 5.22 ms after fault occurrence. Moreover, when it is implemented into a TMS320C6701 DSP, the algorithm performs successfully with the same threshold value of 5% although the errors are increased more than the simulation.

The proposed relay requires no hysteresis data and can reduce the operating time of a relay because it operates in the time domain.

Acknowledgements

Authors would like to thank Korea Ministry of Science and Technology and Korea Science and Engineering Foundation for their support through ERC program.

References

[1] *Applied Protective Relaying*, Westinghouse Electric Corporation, USA, 1976.

[2] Y. Ohura, T. Matsuda, M. Suzuki, M. Yamaura, Y. Kurosawa, and T. Yokoyama, "Digital distance relay with improved characteristics against distorted transient waveforms," *IEEE Trans on PWRD*, vol. 4, no. 4, pp. 2025–2031, October 1989.

[3] A.G. Phadke, and J.S. Thorp, "A New Computer-Based Flux-Restrained Current-Differential Relay for Power Transformer Protection," *IEEE Trans. on PAS*, vol.102, no. 11, pp. 3624–3629, November 1983.

[4] K. Inagaki, M. Higaki, Y. Matsui, K. Kurita, M. Suzuki, K. Yoshida, and T. Maeda, "Digital Protection Method for Power Transformers Based on an Equivalent Circuit Composed of Inverse Inductance," *IEEE Trans. on PWRD*, vol. 3, no. 4, pp. 1501–1510, October 1988.

[5] M.S. Sachdev, T.S. Sidhu, and H.C. Wood, "A Digital Relaying Algorithm for Detecting Transformer Winding Faults," *IEEE Trans. on PWRD*, vol. 4, no. 3, pp. 1638–1648, July 1989.

[6] Y.C. Kang and B.E. Lee, "A Transformer Protective Relaying Algorithm Using the Ratio of Induced Voltages," *KIEE Trans A*, vol. 50, no. 6, pp. 524–530, October 2000.

[7] P. Bastard, P. Bertrand, and M. Meunier, "A Transformer Model for Winding Fault Studies," *IEEE Trans. on PWRD*, vol. 9, no. 2, pp. 690–699, April 1994.

[8] Electromagnetic Transients Program Reference Manual, EMTP Theory Book, 1986, Chapter 2.

Yong-Cheol Kang

He received the B.S., M.S., and Ph.D. degrees from Seoul National University, Seoul, Korea, in 1991, 1993, and 1997, respectively. He was a visiting scholar at Bath University in 1994. He is now an assistant professor at Chonbuk National University, Chonju, Korea. His research interest is development of new protection schemes for power systems using digital signal processing techniques.

Byung-Eun Lee

He received the B.S. and M.S. degrees from Chonbuk National University, Korea, in 1999 and 2001, respectively. He is now studying for his Ph.D. degree at Chonbuk National University. His research interest is power system protection.